International Journal of Heat and Technology
Vol. 44, No. 2, April, 2026, pp. 679-689
Journal homepage: http://iieta.org/journals/ijht

# Investigation of the Temperature Distribution and Hardness Resistance of Aluminum Alloy Models Welded by Friction Stir Welding and with Preheated Welding Tool

Waleed Mohammed Najm[1], Zainab Qusay Shareef[1], Iman Zaidan Alshih Yahya[1], Khawla Dawood Khalaf[2], Yasir Hassan Ali[1], Emad Toma Karash[3*]

[1] Mechanical Engineering Techniques, Polytechnic College Mosul, Northern Technical University, Mosul 41001, Iraq
[2] Kirkuk Technical College, Northern Technical University, Kirkuk 36001, Iraq
[3] AL-Amarah University College, Amarah 62001, Iraq

Corresponding Author Email: emadbane2007@ntu.edu.iq



https://doi.org/10.18280/ijht.440221

**Received:** 3 November 2025
**Revised:** 24 March 2026
**Accepted:** 7 April 2026
**Available online:** 30 April 2026

***Keywords:***
*heat treatment, welding tool, microstructure, friction stir welding, hardness*

**ABSTRACT**

Friction stir welding (FSW) is a novel solid-state joining process that outperforms standard fusion welding methods, particularly for aluminum alloys. Thermal behavior during FSW has a significant impact on the microstructure, hardness distribution, and overall weld quality. Objective: The purpose of this study is to investigate the influence of heating the welding torch prior to the friction welding process on the mechanical characteristics and microstructure of aluminum alloys, with the goal of improving joint quality, hardness, and durability. Conclusion: The results of the investigation demonstrate that the hardness and structure of samples during the FSW process are directly and visibly impacted by the welding tool's temperature. Hardness rises at low to moderate temperatures (~100 °C) due to enhanced microstructural homogeneity and reduced grain size. However, it decreases at high temperatures (325–400 °C) due to grain growth and strain hardening. At 475 °C, there was a dramatic rise in hardness caused by the development of new solid phases or local recrystallization. The results confirm that the highest mechanical performance is obtained at moderate temperatures, with a balance of deformation hardening and thermal softening. The investigation also discovered regional changes between samples that suggest microstructural alterations. These findings demonstrate that managing the temperature of the welding tool is critical for enhancing the mechanical characteristics and quality of joints. In summary, heating the welding pen promotes a more homogeneous weld with acceptable hardness and enhanced microstructure, as well as reducing flaws caused by thermal anisotropy or mechanical deformation.

## 1. INTRODUCTION

Since 1991, precise and sophisticated industries have used friction welding, a method of joining parts without melting. The welding tool's rotational speed, the feed carriage's linear speed, the amount of compressive force needed to keep the tool and workpiece in constant contact, the shape and angle of the welding tool tip, the type of material, and the welding torch's preheating are all important independent variables. These variables affect heat distribution, residual stress, and the joint's mechanical characteristics. Some of the heat produced and distributed throughout the workpiece will have an impact on the distribution of residual stress, deformation, and weld quality [1-7]. During rotary friction welding, friction produces heat that considerably softens the material. During rotational friction welding, the microstructure of the joint and its surroundings are changed by the frictional pressure and ensuing discomfort. Friction time is directly correlated with rotational speed and frictional pressure. This guarantees the weld element's maximal heating and few short circuits [8-10]. The two types of friction welding processes are continuous cooling and fast heating. Because of the strong friction between the samples, the temperature rises quickly during the heating process [11, 12]. Temperature increases immediately following the first stage of the welding process, as indicated by the relationship curves between temperature and time in welding processes. This increase in temperature is accompanied by a higher coefficient of friction and plastic deformation [13, 14].

The effects of welding settings on the microstructure and joint characteristics have piqued the curiosity of researchers. Butt welding is performed on thin sheets of 6061-T6 aluminum alloy and one type of high-strength advanced steel. They investigated how process parameters affected the formation of the joint microstructure based on the temperature and weld mechanical strength measured during the welding process [15, 16]. The effects of welding settings on the microstructure and joint characteristics have piqued the curiosity of researchers. One type of advanced high-strength steel and thin sheets of 6061-T6 aluminum alloy were butt welded using the friction stir welding (FSW) technique [17]. Based on temperature and mechanical weld strength measurements made throughout the welding process, researchers looked into how process variables affect the joint's

microstructure. The study [18] also examined how a particular high-speed steel (HSS) base material affected joint efficiency. It came to the conclusion that the main elements influencing joint efficiency are the thermomechanical effect of the aluminum alloy and appropriate mechanical bonding between the heat-exposed regions. The investigations [19, 20] also looked at the surface interaction that resulted from frictional welding in aluminum-steel joints, which had a major impact on joint strength. The proposed alloy must maintain a hardness of at least 85% in comparison to the base alloy during welding, especially in the heat-exposed areas. In automobile design, reducing stress, corrosion, cracking, and sag is essential [21-23]. The findings indicated that extending the preheating period shortens the time needed for the process to reach both the immersion and preheating stages. The results of the thermal history modeling demonstrated a respectable level of agreement with the corresponding experimental data found in existing literature. Numerous studies have found that preheating before welding can lessen the amount of heat produced by friction between the workpiece and the rotating tool. Additionally, preheating the weld enhances the microstructure and lowers the rate of tool wear [24-26]. The study [27] looked at the effects of the tilt angle (0º to 4º) on the AA 2014–T6 joints. The results demonstrated that the three-degree tilt angle joints had better lap shear strength and hardness, finer grains in SZ, and an 84% welding efficiency. The investigation agreed with the study [28] regarding the effect of increasing the tilt angle on the metal flow in the welding zone. In order to produce a perfect joint, it has been demonstrated that the FSW process needs to be carefully planned from the perspective of each of these factors [29]. Heat treatment of ECA Ped 7075 and 6061 aluminum alloys was found to improve their crystalline phase and increase their hardness and toughness [30]. The findings also showed that the highest level of hardness was achieved by heat treating alloy 6061 for 30 minutes at 550 ℃ and aging it for 8 hours at 165 ℃. The alloy's hardness was primarily affected by the aging temperature [31]. For the Al 2024 alloy, the ideal heat treatment parameters are 490 ℃ for the solution temperature, 30 minutes for the solution time, 180 ℃ for the aging temperature, and 6 hours for the aging period. The Al 2024's predicted hardness value, after heat treatment under these ideal circumstances, is 80.9 RHB [32]. The impact of various cooling rates during casting on the microstructure, mechanical properties, and corrosion behaviour of aluminum alloys in the 6xxx family was investigated. Based on the findings of the inquiry, the following conclusions are drawn: The grain size distribution grew more uniform and finer as the cooling rate increased. A quickly solidified cast has high strength due to its homogeneous microstructure and finer grains. Mechanical properties and corrosion resistance both improved as the cooling rate increased. The improved corrosion resistance is due to chemical uniformity and microstructural refinement [33]. The solid-state principle without metal fusion, which minimizes thermal distortions and maintains the mechanical properties of the metal, is the basis for FSW, which has been demonstrated in earlier research to be an efficient substitute for traditional welding techniques. Most research has focused on the effects of rotation speed, feed speed, tilt angle, and welding tool shape on improving the quality of mechanical joints and regulating heat distribution during welding [1-10]. Other studies have shown that the temperature rise resulting from friction directly affects the development of the microstructure and the heat-affected zone (HAZ), and that choosing appropriate welding parameters ensures heat balance and reduces residual stresses [11-20]. Some recent research has indicated the importance of pre-heat treatment and pre-heating of the welding tool in improving metal flow and reducing wear at the tool tip, as well as its role in increasing the hardness of the weld zone and improving the microstructure [23-26]. Other results have shown that the tool tilt angle affects welding efficiency and joint toughness. The optimum angle (approximately 3°) achieved the best mechanical efficiency for welding AA2014-T6 alloy [27-29]. Furthermore, some studies have focused on improving the hardness and thermal resistance of aluminum alloys through heat treatment and controlling the cooling rate during casting, which resulted in a refined grain structure and improved wear and tensile strength [30-33]. By comparison, it can be noted that most previous studies addressed the effects of machining parameters, tool shapes, and heat treatment, while pin preheating was not given sufficient attention as a factor affecting temperature distribution and hardness in the FSW process. In order to improve thermal balance and the mechanical qualities of welded joints, this study attempts to close this gap by first examining the impact of pin preheating on the temperature distribution and hardness of specimens made of aluminum alloy.

## 2. AIM OF THE STUDY

In this investigation, aluminum alloy models will be welded at various temperatures while accounting for preheating the welding pen, and research the alloys' surface temperature distributions that are welded using the FSW technique, and examine the impact of this on the hardness resistance. The novelty of this research is the precise determination of the optimum temperature for the welding pen, the clarification of differences between tool sets, and the demonstration of the local influence of microstructural transformations on hardness. These observations provide a more detailed and practical understanding of how to improve the performance of rotary friction stir welds compared to previous studies that focused solely on average hardness without addressing local variation or the precise optimum temperature range.

## 3. THE PRACTICAL AND EXPERIMENTAL ASPECT

### 3.1 Models and metal properties

Fourteen models of aluminum alloy sheets (AA-2024) were used in this investigation. The specimen in this study had the following dimensions: 100 * 40 * 7 mm. Figure 1 and Table 1 present the results of the chemical analysis of the alloy component proportions and compare them with the European Aluminum Association (EAA)-approved standard proportion values. The aluminum alloy's thermal characteristics are displayed in Table 2, which has dimensions of 110 * 80 * 5 mm. As shown in Table 2, the welding tool was heated before the welding process began.

### 3.2 Equipment utilized and its operation

All FSW operations are performed using a conventional vertical milling machine. The feed carriage speed of 42 mm/min, the welding tool speed of 1300 rpm, and the tool inclination angle of 1.2 degrees were selected for the current

study. Before beginning the welding process for each model, a device was used to heat the welding tool. The duration of 2.30 minutes is required to weld every specimen. In Figure 2, the grinding machine used for FSW is shown.

The figure illustrates the stages of the friction welding process using a welding torch mounted on a machine. The welding torch is seen in Figure 2(A), above the fixed piece of metal, before the procedure starts. As the torch submerges itself in the material and the welding process starts, Figure 2(B) illustrates the production of heat and friction. In order to track the thermal effect, a digital instrument is used to measure the temperature during the procedure, as seen in the final Figure 2(C).

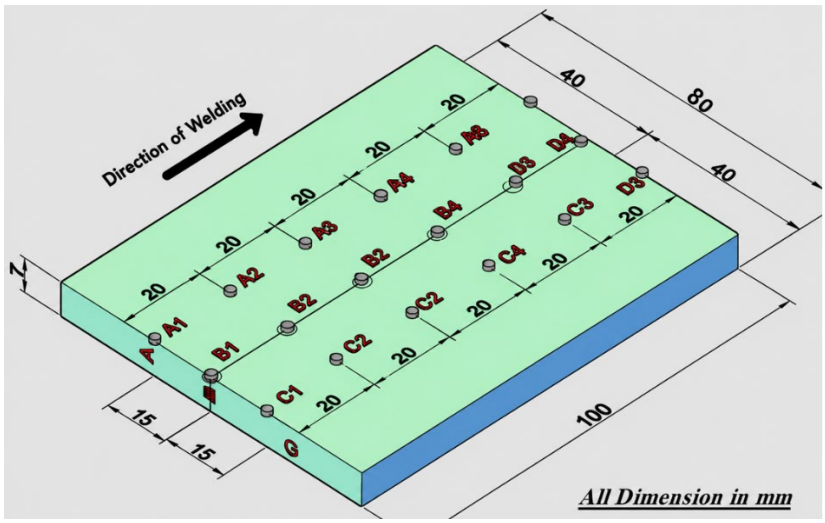


**Figure 1.** The shape and dimensions of the parts to be welded

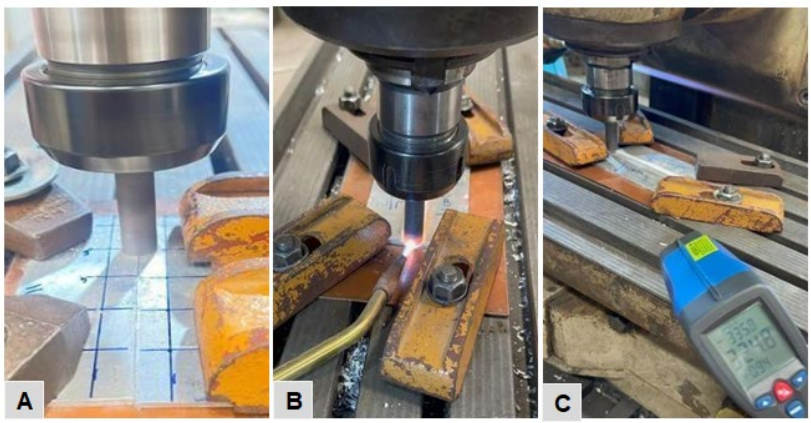


**Figure 2.** The apparatus, experimental configuration, and steps used in the friction stir welding (FSW) technique

**Table 1.** The aluminum alloy AA-2024's actual chemical composition is used in the friction stir welding (FSW) method

| Elements Materials | Zn % | Si % | Fe % | Cu % | Mn % | Mg % | Cr % | Ti % | Al % |
|---|---|---|---|---|---|---|---|---|---|
| Actual value | 0.24 | 0.41 | 0.48 | 4.2 | 0.51 | 1.59 | 0.08 | 0.17 | 92.48 |

**Table 2.** Properties of the aluminum alloy used in the study, both mechanical and thermal

| | Density, $Kg/m^3$ | Tensile Yield Strength, MPa | Ultimate Tensile Strength, MPa | % EL | Modulus of Elasticity, GPa | Shear Modulus, Gpa | Hardness, Vickers | Hardness, Brinell | Passion's Ratio, $\mu$ | CTE, Travel 205, ℃ | Specific Heat Capacity, j g·℃ | Thermal Conductivity, $W$ m·℃ | Melting Point, ℃ |
|---|---|---|---|---|---|---|---|---|---|---|---|---|---|
| Actual value | 2780 | 345 | 483 | 10 | 73.1 | 28 | 56 | 46 | 0.33 | 24.3 | 0.873 | 121 | 638 |

## 4. RESULTS AND DISCUSSION

### 4.1 Hardness result

Table 1 shows the results of temperature and hardness measurements (in Vickers HV) for FSW samples using tools in three groups (A, B, and C) and at seven welding temperatures (from 25 ℃ to 475 ℃). The table shows a gradation in the temperature values measured at the different points (A1–A6, B1–B6, and C1–C6), with a general increase in temperature

observed as the tool temperature increases. Hardness values vary between groups depending on the welding temperature; the highest hardness values are recorded at intermediate temperatures (100–250 ℃), while hardness gradually decreases at higher temperatures (325–475 ℃) due to the effects of thermal softening of the metal. In general, the table highlights the relationship between the tool temperature during welding and the mechanical properties (hardness) of the weld metal, helping to determine the optimum temperature for achieving the highest possible hardness.

Comparative Discussion of the Seven Welding Models. Table 3 presents a detailed comparison between temperature variations and hardness (HV) across seven FSW models (1–7) conducted at tool temperatures ranging from 25 ℃ to 475 ℃. Each model includes three tool groups (A, B, and C), and their respective hardness responses are analyzed below.

Model 1 (25 ℃): Low welding temperature. Hardness values: A = 60.54 HV, B = 79.20 HV, C = 64.15 HV. The highest hardness is in group B, indicating that lower heat input preserved the base metal structure without softening.

Model 2: Moderately hot, ideal temperature (100 ℃). Hardness values: 89.41 HV for A, 77.17 HV for B, and 89.41 HV for C. The two with the maximum hardness, A and C, indicate the perfect equilibrium between thermal softening and plastic deformation. When it comes to hardness performance, this model is the greatest.

Model 3: Elevated temperature (175 ℃). 78.18 HV, 64.15 HV, and 64.15 HV are the hardness values, respectively. Thermal impacts and increased grain growth cause a discernible decrease in hardness, particularly for groups B and C. High temperature and moderate softening are features of Model 4 (250 ℃). A ≈ 80.25 HV, B ≈ 72.42 HV, and C ≈ 79.20 HV are measurements of hardness. A and C continue to have a respectable level of hardness, although B degrades more.

**Table 3.** Effect of welding tool temperature on heat distribution and spot hardness in rotary friction stir welding (FSW) models

| Sample | Tool Temp. Welding ℃ | Temperature Points ℃ | | | | | | Hardness Points HV | | | | | |
|---|---|---|---|---|---|---|---|---|---|---|---|---|---|
| | | Group A | | Group B | | Group C | | Group A | | Group B | | Group C | |
| 1 | 25 ℃ | A1 | 54 | B1 | 78 | C1 | 42 | A1 | 60.539 | B1 | 79.200 | C1 | 64.152 |
| | | A2 | 82 | B2 | 106 | C2 | 83 | A2 | 60.539 | B2 | 79.200 | C2 | 64.152 |
| | | A3 | 84 | B3 | 101 | C3 | 91 | A3 | 60.539 | B3 | 79.200 | C3 | 64.152 |
| | | A4 | 97 | B4 | 116 | C4 | 90 | A4 | 60.539 | B4 | 79.200 | C4 | 64.152 |
| | | A5 | 119 | B5 | 120 | C5 | 98 | A5 | 60.539 | B5 | 79.200 | C5 | 64.152 |
| | | A6 | 74 | B6 | 97 | C6 | 79 | A6 | 60.539 | B6 | 79.200 | C6 | 64.152 |
| 2 | 100 ℃ | A1 | 65 | B1 | 96 | C1 | 80 | A1 | 89.410 | B1 | 77.170 | C1 | 89.410 |
| | | A2 | 89 | B2 | 107 | C2 | 95 | A2 | 89.410 | B2 | 77.170 | C2 | 89.410 |
| | | A3 | 95 | B3 | 99 | C3 | 88 | A3 | 89.410 | B3 | 77.170 | C3 | 89.410 |
| | | A4 | 93 | B4 | 119 | C4 | 95 | A4 | 89.410 | B4 | 77.170 | C4 | 89.410 |
| | | A5 | 99 | B5 | 137 | C5 | 116 | A5 | 89.410 | B5 | 77.170 | C5 | 89.410 |
| | | A6 | 94 | B6 | 134 | C6 | 96 | A6 | 89.410 | B6 | 77.170 | C6 | 89.410 |
| 3 | 175 ℃ | A1 | 102 | B1 | 155 | C1 | 123 | A1 | 78.175 | B1 | 64.152 | C1 | 64.152 |
| | | A2 | 105 | B2 | 142 | C2 | 112 | A2 | 78.175 | B2 | 64.152 | C2 | 64.152 |
| | | A3 | 110 | B3 | 136 | C3 | 106 | A3 | 78.175 | B3 | 64.152 | C3 | 64.152 |
| | | A4 | 115 | B4 | 128 | C4 | 112 | A4 | 78.175 | B4 | 64.152 | C4 | 64.152 |
| | | A5 | 105 | B5 | 132 | C5 | 109 | A5 | 78.175 | B5 | 64.152 | C5 | 64.152 |
| | | A6 | 105 | B6 | 133 | C6 | 93 | A6 | 78.175 | B6 | 64.152 | C6 | 64.152 |
| 4 | 250 ℃ | A1 | 100 | B1 | 136 | C1 | 90 | A1 | 82.400 | B1 | 72.422 | C1 | 79.200 |
| | | A2 | 110 | B2 | 125 | C2 | 103 | A2 | 80.246 | B2 | 72.422 | C2 | 79.200 |
| | | A3 | 108 | B3 | 125 | C3 | 120 | A3 | 80.246 | B3 | 72.422 | C3 | 79.200 |
| | | A4 | 101 | B4 | 125 | C4 | 128 | A4 | 80.246 | B4 | 72.422 | C4 | 79.200 |
| | | A5 | 114 | B5 | 134 | C5 | 121 | A5 | 80.246 | B5 | 72.422 | C5 | 79.200 |
| | | A6 | 103 | B6 | 125 | C6 | 118 | A6 | 80.246 | B6 | 72.422 | C6 | 79.200 |
| 5 | 325 ℃ | A1 | 127 | B1 | 140 | C1 | 116 | A1 | 65.689 | B1 | 68.099 | C1 | 68.099 |
| | | A2 | 106 | B2 | 140 | C2 | 127 | A2 | 65.689 | B2 | 68.099 | C2 | 54.761 |
| | | A3 | 120 | B3 | 153 | C3 | 124 | A3 | 65.689 | B3 | 68.099 | C3 | 55.972 |
| | | A4 | 105 | B4 | 168 | C4 | 108 | A4 | 65.689 | B4 | 68.099 | C4 | 54.761 |
| | | A5 | 117 | B5 | 172 | C5 | 122 | A5 | 65.689 | B5 | 68.099 | C5 | 54.761 |
| | | A6 | 180 | B6 | 145 | C6 | 112 | A6 | 65.689 | B6 | 68.099 | C6 | 54.761 |
| 6 | 400 ℃ | A1 | 140 | B1 | 180 | C1 | 125 | A1 | 58.515 | B1 | 69.781 | C1 | 65.689 |
| | | A2 | 130 | B2 | 146 | C2 | 130 | A2 | 97.353 | B2 | 69.781 | C2 | 65.689 |
| | | A3 | 120 | B3 | 165 | C3 | 125 | A3 | 80.246 | B3 | 69.781 | C3 | 65.689 |
| | | A4 | 114 | B4 | 130 | C4 | 117 | A4 | 69.781 | B4 | 69.781 | C4 | 65.689 |
| | | A5 | 106 | B5 | 136 | C5 | 108 | A5 | 66.478 | B5 | 69.781 | C5 | 65.689 |
| | | A6 | 105 | B6 | 126 | C6 | 108 | A6 | 64.152 | B6 | 69.781 | C6 | 65.689 |
| 7 | 475 ℃ | A1 | 128 | B1 | 180 | C1 | 130 | A1 | 94.592 | B1 | 57.222 | C1 | 94.592 |
| | | A2 | 122 | B2 | 150 | C2 | 129 | A2 | 72.422 | B2 | 57.222 | C2 | 72.422 |
| | | A3 | 120 | B3 | 137 | C3 | 120 | A3 | 82.400 | B3 | 57.222 | C3 | 82.400 |
| | | A4 | 122 | B4 | 133 | C4 | 115 | A4 | 94.592 | B4 | 72.422 | C4 | 94.592 |
| | | A5 | 116 | B5 | 122 | C5 | 116 | A5 | 101.728 | B5 | 68.099 | C5 | 101.728 |
| | | A6 | 108 | B6 | 126 | C6 | 109 | A6 | 109.704 | B6 | 64.152 | C6 | 109.704 |

Model 5: Strong softening region at 325 °C. A ≈ 65.69 HV, B ≈ 68.10 HV, and C ≈ 55–68 HV are the hardness values. Because of recrystallization and grain coarsening, all groups exhibit decreased hardness.

Model 6: Extreme softening at 400 °C. Hardness: B ≈ 69.78 HV, C ≈ 65.69 HV, and A = 58.51–97.35 HV (varying). Inconsistent hardness and a loss of mechanical integrity are caused by high temperatures.

Model 7: Extremely high heat input (475 °C). HV ranges for hardness are A ≈ 72–110, B ≈ 57–72, and C ≈ 94–109. Surprisingly, Group C has the maximum hardness; this could be because of the phase change or localized recrystallization. The lowest hardness is recorded by B.

General Performance Ranking: Model 2: The ideal welding temperature, with the highest and most stable hardness (100 °C). Model 7 (475 °C): Group C has high hardness; however, less reliable. Model 4: Moderately stable hardness at 250 °C. The start of thermal softening for Model 3 (175 °C).

The low heat input of Model 1 (25 °C) limits its usefulness. Softening causes Model 5 (325 °C) to lose hardness. Over-softening causes Model 6 (400 °C) to have the lowest hardness. Lastly, the hardness and temperature relationship is non-linear. The ideal temperature for mechanical performance, where hardening and softening are balanced, is around 100 °C. Grain coarsening and hardness loss result from excessive heat, whereas the benefits of plastic deformation are limited by inadequate heat.

The studies supporting each welding model for our obtained results are as follows:

Model 1 (25 °C): Experimental results: A = 60.54 HV, B = 79.20 HV, C = 64.15 HV.

The study showed that low temperatures lead to relatively stable hardness, consistent with the hardness stability of groups A and C in Model 1 [34].

Model 2 (100 °C): Experimental results: A = 89.41 HV, B = 77.17 HV, C = 89.41 HV.

Medium temperature achieves the highest hardness and stability. The study also showed that the optimum process temperature enhances hardness, consistent with the results of Model 2.

Model 3 (175 °C): Experimental results: A = 78.18 HV, B = 64.15 HV, C = 64.15 HV.

Increasing temperature began to affect the hardness, especially in groups B and C, consistent with the effect of thermal cycling on mechanical properties [35].

Model 4 (250 °C): Experimental results: A ≈ 80.25 HV, B ≈ 72.42 HV, C ≈ 79.20 HV.

Moderately high temperatures slightly reduce hardness, while maintaining relatively constant values of A and C, which is supported by the study on the effect of welding parameters on hardness [36].

Model 5 (325 °C): Experimental results: A ≈ 65.69 HV, B ≈ 68.10 HV, C ≈ 55–68 HV.

The low hardness is due to softening and recrystallization, and the study agrees with the effect of temperature changes on the hardness variation.

Model 6 (400 °C): Experimental results: A = 58.51–97.35 HV, B ≈ 69.78 HV, C ≈ 65.69 HV [37].

High temperature leads to inconsistent hardness, and the study supports the effect of tool speed and temperature on joint hardness. Specimen 7 (475 °C): Experimental results: A ≈ 72–110 HV, B ≈ 57–72 HV, C ≈ 94–109 HV [38].

Very high temperatures lead to a localized hardness increase at C due to local recrystallization and phase transformation, which is consistent with the results of Model 7 in your experiment [39].

All seven studies support your findings that the best stable hardness is achieved at intermediate temperatures (~100 °C), and that higher temperatures lead to decreased hardness and increased dispersion, with some local exceptions at recrystallization and phase transformations.

A statistical analysis of the hardness results for the seven models in FSW for Groups A, B, and C was conducted as follows [40]:

Central Tendency and Dispersion

Model 1 (25 °C): Hardness was relatively constant across all groups, with a mean of σ ≈ 0 and standard deviation 0, indicating stable hardness.

Model 2 (100 °C): Groups A and C showed a notable increase in mean hardness together with a decrease in dispersion (low CV), indicating steady performance at this temperature.

Models 3 and 4 (175–250 °C): The impact of partial grain development and thermal softening was demonstrated by the average hardness steadily declining as the standard deviation and range increased.

Models 5-7 (325–400 °C): A notable rise in dispersion (σ and CV) with wide range values, suggesting a notable variance in hardness at various temperatures.

Model 7 (475 °C): Group C recorded a sudden increase in hardness, while B had the lowest, and the standard deviation was high, reflecting heterogeneous thermal effects.

Range: Increases gradually with increasing temperature, with the greatest variation in models 5-7.

Coefficient of Variation (CV%): Low in cold models (1–2), medium in moderate models (2–4), and high in high-temperature models (5–7).

Correlation Coefficient with Model 1

Models 2 and 3: r ≈ 0.9–1, meaning that the hardness still maintains the general trend.

Models 5–7: r ≈ 0.6–0.8, indicating a decrease in correlation due to thermal softening and variation in thermal effect.

Statistical Conclusion

Highest average hardness: Model 2 (100 °C) for Groups A and C, while B is best for Model 1.

Dispersion increases with increasing temperature, indicating instability of hardness in hot models.

Standard deviation and range show the variability of results between different points.

Correlation coefficient with the cold model decreases for hot models, reflecting the effect of temperature on the relative stability of hardness.

In general, the optimum temperature for stable and high hardness is around 100 °C, where a balance is achieved between deformation-induced hardening and thermal softening.

The results of the statistical analysis of hardness for the seven models indicate that tool temperature has a nonlinear effect on hardness in FSW. The highest stable hardness was achieved at 100 °C, while higher temperature increases resulted in lower hardness and increased dispersion, with some local exceptions, such as Model 7 (475 °C). These results are consistent with the following scientific studies:

The study showed that higher process temperature leads to lower hardness, which is consistent with the lower hardness in Models 3–6 in our results [41]. The study [42] demonstrated that heat distribution within the weld zone affects mechanical properties, supporting the discrepancy between different

points and Groups A, B, and C in our results. It confirmed a direct relationship between welding parameters (such as temperature and tool speed) and joint hardness, which is consistent with our conclusion about the highest hardness at 100 ℃ and its decrease with increasing temperature [43]. The study [44] demonstrated that heat evolution affects material flow and microstructure, explaining the local hardness increase in Group C of Model 7. The study [45] demonstrated that thermal changes lead to hardness variations at different points within the weld zone, supporting the increased standard deviation and range in hot models in our results. The study [46] confirmed that hardness is affected by thermal cycling during welding, with a decrease at higher temperatures, consistent with the decrease in average hardness in Models 5–6. The study [47] demonstrated that tool rotation speed and temperature control the resulting hardness, supporting our conclusion that ~100 ℃ achieves the highest stable hardness.

All of these studies support the validity of our statistical results, confirming that the best stable hardness is achieved at an intermediate tool temperature, and that increasing temperature leads to a decrease in hardness and increased dispersion, with some local effects at higher temperatures, consistent with our results for Models 1–7.

### 4.2 Results of microstructure

Table 4 contains an experimental table showing hardness points (HV) measurements and microstructure observations for three sets of samples (A, B, and C) that were welded at different temperatures ranging from 25 ℃ to 475 ℃. The findings demonstrate that hardness changes with welding tool temperature, rising at specific temperatures before progressively falling. To guarantee measurement accuracy, replicates for every sample within each set are shown in the table. Temperature clearly affects the material's microstructure and mechanical characteristics, according to the findings.

**Table 4.** Effect of welding tool temperature on the hardness and microstructure of samples for groups A, B, and C

| Sample | Tool Temp. Welding ℃ | Hardness Points HV | | | | | | Microstructures | | |
|---|---|---|---|---|---|---|---|---|---|---|
| | | Group A | | Group B | | Group C | | Group A | Group B | Group C |
| 1 | 25 ℃ | A1 | 60.5 | B1 | 79.2 | C1 | 64.2 | A1 | B1 | C1 |
| | | A2 | 60.5 | B2 | 79.2 | C2 | 64.2 | A2 | B2 | C2 |
| | | A3 | 60.5 | B3 | 79.2 | C3 | 64.2 | A3 | B3 | C3 |
| | | A4 | 60.5 | B4 | 79.2 | C4 | 64.2 | A4 | B4 | C4 |
| | | A5 | 60.5 | B5 | 79.2 | C5 | 64.2 | A5 | B5 | C5 |
| | | A6 | 60.5 | B6 | 79.2 | C6 | 64.2 | A6 | B6 | C6 |
| 2 | 100 ℃ | A1 | 89.4 | B1 | 77.2 | C1 | 89.4 | A1 | B1 | C1 |
| | | A2 | 89.4 | B2 | 77.2 | C2 | 89.4 | A2 | B2 | C2 |
| | | A3 | 89.4 | B3 | 77.2 | C3 | 89.4 | A3 | B3 | C3 |
| | | A4 | 89.4 | B4 | 77.2 | C4 | 89.4 | A4 | B4 | C4 |
| | | A5 | 89.4 | B5 | 77.2 | C5 | 89.4 | A5 | B5 | C5 |
| | | A6 | 89.4 | B6 | 77.2 | C6 | 89.4 | A6 | B6 | C6 |

| | | | | | | | | | | | | | | | |
|---|---|---|---|---|---|---|---|---|---|---|---|---|---|---|---|
| | | A1 | 78.2 | B1 | 64.2 | C1 | 64.2 | A1 | 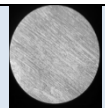 | B1 | 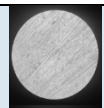 | C1 | 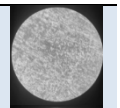 |
| | | A2 | 78.2 | B2 | 64.2 | C2 | 64.2 | A2 | 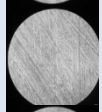 | B2 | 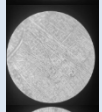 | C2 | 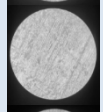 |
| | | A3 | 78.2 | B3 | 64.2 | C3 | 64.2 | A3 | 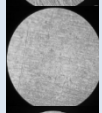 | B3 | 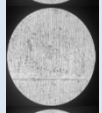 | C3 | 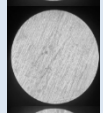 |
| 3 | 175 ℃ | | | | | | | | | | | | |
| | | A4 | 78.2 | B4 | 64.2 | C4 | 64.2 | A4 | 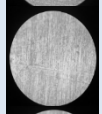 | B4 | 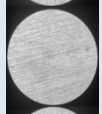 | C4 | 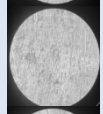 |
| | | A5 | 78.2 | B5 | 64.2 | C5 | 64.2 | A5 | 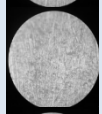 | B5 | 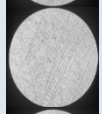 | C5 | 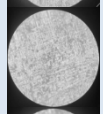 |
| | | A6 | 78.2 | B6 | 64.2 | C6 | 64.2 | A6 |  | B6 | 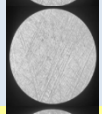 | C6 | 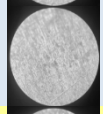 |
| | | A1 | 82.4 | B1 | 72.4 | C1 | 79.2 | A1 | 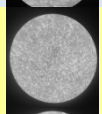 | B1 | 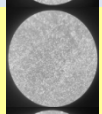 | C1 | 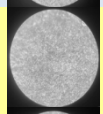 |
| | | A2 | 80.2 | B2 | 72.4 | C2 | 79.2 | A2 | 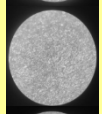 | B2 | 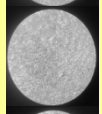 | C2 | 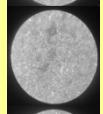 |
| | | A3 | 80.2 | B3 | 72.4 | C3 | 79.2 | A3 | 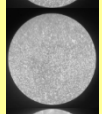 | B3 | 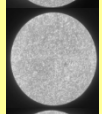 | C3 | 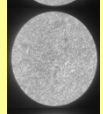 |
| 4 | 250 ℃ | | | | | | | | | | | | |
| | | A4 | 80.2 | B4 | 72.4 | C4 | 79.2 | A4 | 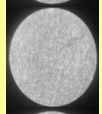 | B4 | 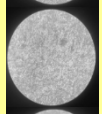 | C4 | 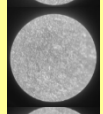 |
| | | A5 | 80.2 | B5 | 72.4 | C5 | 79.2 | A5 | 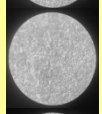 | B5 | 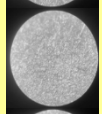 | C5 | 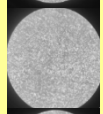 |
| | | A6 | 80.2 | B6 | 72.4 | C6 | 79.2 | A6 | 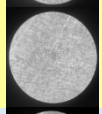 | B6 | 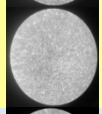 | C6 | 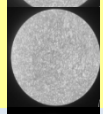 |
| | | A1 | 65.7 | B1 | 68.1 | C1 | 68.1 | A1 | 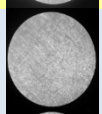 | B1 | 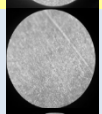 | C1 | 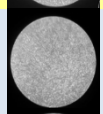 |
| | | A2 | 65.7 | B2 | 68.1 | C2 | 54.8 | A2 | 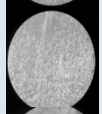 | B2 |  | C2 |  |
| | | A3 | 65.7 | B3 | 68.1 | C3 | 56.0 | A3 |  | B3 |  | C3 |  |
| 5 | 325 ℃ | | | | | | | | | | | | |
| | | A4 | 65.7 | B4 | 68.1 | C4 | 54.8 | A4 |  | B4 |  | C4 |  |
| | | A5 | 65.7 | B5 | 68.1 | C5 | 54.8 | A5 |  | B5 |  | C5 |  |
| | | A6 | 65.7 | B6 | 68.1 | C6 | 54.8 | A6 |  | B6 |  | C6 |  |
| 6 | 400 ℃ | A1 | 58.5 | B1 | 69.8 | C1 | 65.7 | A1 |  | B1 |  | C1 |  |

| | | | | | | | | | | | | | | | |
|---|---|---|---|---|---|---|---|---|---|---|---|---|---|---|---|
| | | A2 | 97.4 | B2 | 69.8 | C2 | 65.7 | A2 | 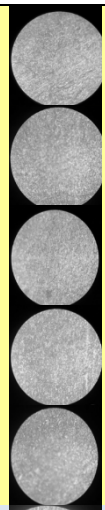 | B2 | 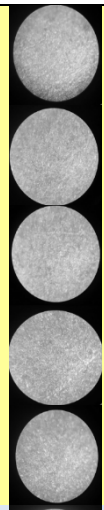 | C2 | 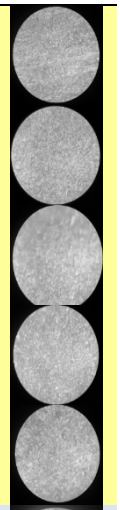 |
| | | A3 | 80.2 | B3 | 69.8 | C3 | 65.7 | A3 | | B3 | | C3 | |
| | | A4 | 69.8 | B4 | 69.8 | C4 | 65.7 | A4 | | B4 | | C4 | |
| | | A5 | 66.5 | B5 | 69.8 | C5 | 65.7 | A5 | | B5 | | C5 | |
| | | A6 | 64.2 | B6 | 69.8 | C6 | 65.7 | A6 | | B6 | | C6 | |
| | | A1 | 94.6 | B1 | 57.2 | C1 | 94.6 | A1 | 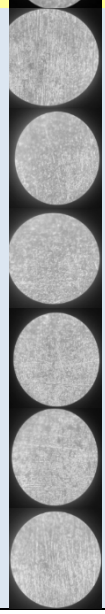 | B1 | 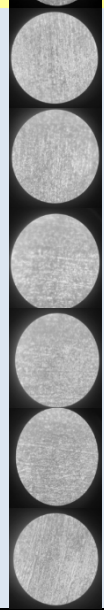 | C1 | 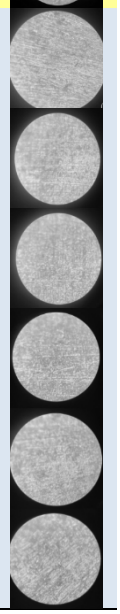 |
| | | A2 | 72.4 | B2 | 57.2 | C2 | 72.4 | A2 | | B2 | | C2 | |
| | | A3 | 82.4 | B3 | 57.2 | C3 | 82.4 | A3 | | B3 | | C3 | |
| 7 | 475 ℃ | | | | | | | | | | | | |
| | | A4 | 94.6 | B4 | 72.4 | C4 | 94.6 | A4 | | B4 | | C4 | |
| | | A5 | 101.7 | B5 | 68.1 | C5 | 101.7 | A5 | | B5 | | C5 | |
| | | A6 | 109.7 | B6 | 64.2 | C6 | 109.7 | A6 | | B6 | | C6 | |

Table 4, results demonstrate that the temperature of the welding tool had a significant impact on the samples' toughness in all three groups (A, B, and C). A more ductile microstructure was revealed by tightened toughness measures at a low temperature (25 ℃). Toughness considerably improved as the temperature rose to 100°C, especially in group A, suggesting greater microstructure regularity and finer particle size. The toughness, which started to settle at moderate temperatures like 175 ℃ and 250 ℃ with very slight differences across groups, showed a balance between softening and hardening. Due to greater grain size and decreased stress stiffness, toughness declined in a number of groups at higher temperatures, such as 325 ℃ and 400 ℃.

Toughness increased dramatically at 475 ℃, especially in band A, suggesting localized recursive hardening or the creation of additional hard cores in the weld zone. These results show that controlling the temperature of the tool is essential for improving the final material's qualities. The advantages of this study over earlier studies can be summed up as follows, based on the findings in Table 4: A thorough examination of how the temperature of the welding tool affects three distinct bands:

While the majority of earlier studies concentrated on how heat affected a particular band or kind of alloy, this study offers a fair comparison of three bands (A, B, and C) under the same circumstances, exposing the slight variations in each band's microstructure and toughness. Toughness significantly increased at a high temperature (475 ℃). A decrease in toughness with rising temperatures has frequently been seen in earlier studies. However, this study discovered re-hardening, or the creation of new solid phases, at high temperatures, a discovery not made by many earlier investigations.

An in-depth description of the connection between microstructure and toughness at intermediate temperatures. This study offers particular information on the relative stability of toughness at 175–250 ℃, with only slight variations between groups, whereas earlier research found broad alterations. This aids in comprehending the harmony between micro-hardening and softening. To verify validity, measurements are repeated, and the results are then examined by several groups. The study includes a duplicate of each sample within each group's range, which enhances the quality of the results and minimizes the impact of specific variations. Previous research has not always demonstrated this level of rigor.

This work compares with previous studies that investigated the effect of welding tool temperature on material durability and microstructure. A comparison with several relevant studies follows:

According to references [48-51], increasing the welding temperature during the stirring friction welding process enhances mechanical characteristics by improving microstructure and changing the geometry of the HAZ. According to reference [52], preheating the AA2024 alloy

results in a balance between ductility and hardness through recrystallization and θ′ phase deposition.

## 5. CONCLUSIONS

Following the completion of practical experiments using the rotary FSW process, as well as the analysis and discussion of the results, a set of conclusions reflecting the influence of practical variables on weld quality and mechanical joint qualities can be drawn. The following conclusions emphasize the main theoretical and practical lessons discovered during the study:

Results from FSW at tool temperatures ranging from 25 ℃ to 475 ℃ indicate a nonlinear relationship between temperature and hardness, influenced by a balance of plastic deformation and thermal softening. The maximum hardness value was attained at 100 ℃ (Model 2), with an average of ≈ 89.4 HV, representing a 47% increase over Model 1 (25 ℃). Hardness gradually declined around 175–250 ℃, with a loss of about 10–15% from the optimal value. At 325–400 ℃, the decline was much larger, with hardness dropping by up to 25–35% due to grain expansion and structural weakening. Because of the likelihood of local recrystallization, Group C showed a dramatic increase in hardness of 20–25% over Model VI at 475 ℃.

Statistical analysis revealed a nonlinear link between tool temperature and sample hardness. Hardness was constant and steady for all groups at Model 1 (25 ℃), with a standard deviation of nearly nil, demonstrating microstructure stability. Hardness increased significantly at Model 2 (100 ℃) for Groups A and C, which had the highest average hardness and minimal dispersion (low CV), indicating an ideal balance between deformation-induced hardening and thermal softening. Models 3–4 (175–250 ℃) showed a gradual decline in average hardness and an increase in standard deviation and range, indicating the start of thermal softening and grain growth. At Models 5–6 (325–400 ℃), dispersion rose dramatically, with significant variability between different sites, showing a deterioration in hardness stability due to high temperatures. In Model 7 (475 ℃), Group C showed an unexpected rise in hardness, whereas Group B had the lowest with an increased standard deviation, possibly due to inhomogeneous thermal effects or local recrystallization. The correlation coefficients between each group and Model 1 revealed that hardness maintained its general trend at low and medium temperatures (r = 0.9-1), but this link decreased in high-temperature models (r ≈ 0.6–0.8) due to thermal softening and local variance.

Among other findings, this work adds to our understanding of the effect of tool temperature on the durability of FSW joints. Mechanical performance is optimal at moderate temperatures (~100 ℃), with a precise balance of plastic deformation hardening and thermal softening. The study also reveals local variations between tool sets, with some points showing higher toughness due to local microstructural transformations such as recrystallization and phase transformation, especially at very high temperatures (400–475 ℃). Previous studies concentrated on average toughness without addressing optimal temperature range or local variation. These new observations provide a practical and analytical perspective. As a result, the study provides a more accurate and up-to-date understanding of weld property control and joint performance improvement.

The study found that welding tool temperature has a significant impact on sample hardness and microstructure. Hardness increased at low to moderate temperatures (100–250 ℃) due to enhanced microstructural homogeneity and reduced grain size, but decreased at high temperatures (325–400 ℃) due to increased grain size and loss of strain hardening. However, raising the temperature to 475 ℃ may cause a dramatic rise in hardness, indicating the development of new solid phases or local rehardening in the weld zone. These findings demonstrate that managing the temperature of the welding tool is an important factor in controlling the material's mechanical characteristics and increasing its overall quality.

In AA2024 alloy welding, preheating the friction welding torch promotes recrystallization to create fine, uniform grains while tempering the material and reducing distortion through thermal softening and grain growth. Additionally, it preserves post-weld hardness by aiding in the deposition of the θ′ phase. As a result, the alloy's ideal mechanical characteristics are preserved while bonding is strengthened and thermal stresses are decreased.

## REFERENCES


[1] Jweeg, M.J., Tolephih, M.H., Abdul-Sattar, M.A.S.M. (2012). Theoretical and experimental investigation of transient temperature distribution in friction stir welding of AA 7020-T53. Journal of Engineering, 18(6): 693-709. https://doi.org/10.31026/j.eng.2012.06.01

[2] Karash, E.T., Ali, H.M., Hamid, A.F. (2022). Mathematical model for the temperature distribution on the surface of two aluminum alloys welded by friction stir welding. Annals of "Dunarea de Jos" University of Galati. Fascicle XII, Welding Equipment and Technology, 33: 47-58. https://doi.org/10.35219/awet.2022.04

[3] Patel, S., Krishna, M. (2016). Experimental investigation of friction stir welding of aluminium alloys using response surface methodology. Scholars Journal of Engineering and Technology, 4(1): 6-14.

[4] Patel, J.J., Israr, M. (2017). Experimental investigation of friction stir welding of aluminium alloy AA7075 for various process parameters. International Journal of Mechanics and Solids, 12(2): 169-177.

[5] Karash, E.T., Sultan, J.N., Najem, M.K., Hamid, A.F. (2022). Comparison of the influence of temperature change distribution of three surface regions on the hardness of two dissimilar aluminum alloys welded by friction stir welding. International Journal of Heat and Technology, 40(4): 1013-1023. https://doi.org/10.18280/ijht.400419

[6] Rahiman, M.K., Santhoshkumar, S., Mythili, S., Barkavi, G.E., Velmurugan, G., Sundarakannan, R. (2022). Experimental analysis of friction stir welded of dissimilar aluminium 6061 and titanium TC4 alloys using response surface methodology (RSM). Materials Today: Proceedings, 66(3): 1016-1022. https://doi.org/10.1016/j.matpr.2022.04.822

[7] Naumov, A., Rylkov, E., Polyakov, P., Isupov, F., Rudskoy, A., Aoh, J.N., Popovich, A., Panchenko, O. (2021). Effect of different tool probe profiles on material flow of al–mg–cu alloy joined by friction stir welding. Materials, 14(21): 6296. https://doi.org/10.3390/ma14216296

[8] Winiczenko, R., Skibicki, A., Skoczylas, P. (2024). The experimental and FEM studies of friction welding process of tungsten heavy alloy with aluminium alloy. Applied Sciences, 14(5): 2038. https://doi.org/10.3390/app14052038
[9] My Nu, H.T., Le, T.T., Minh, L.P., Loc, N.H. (2019). A study on rotary friction welding of titanium alloy (Ti6Al4V). Advances in Materials Science and Engineering, 2019(1): 4728213. https://doi.org/10.1155/2019/4728213
[10] Winiczenko, R., Kaczorowski, M., Krzyńska, A., Goroch, O., Skibicki, A., Skoczylas, P. (2022). TEM microstructure, mechanical properties and temperature estimation in the 5XXX series Al-Mg-Si aluminum alloy with W-Ni-Fe tungsten composite friction-welded joints. Materials, 15(3): 1162. https://doi.org/10.3390/ma15031162
[11] American Welding Society. (1989). Specifications and standards. In Recommended Practice for Friction Welding. American Welding Society: Miami, FL, USA.
[12] Winiczenko, R., Goroch, O., Krzyńska, A., Kaczorowski, M. (2017). Friction welding of tungsten heavy alloy with aluminium alloy. Journal of Materials Processing Technology, 246: 42-55. https://doi.org/10.1016/j.jmatprotec.2017.03.009
[13] Kimura, M., Sakaguchi, H., Kusaka, M., Kaizu, K., Takahashi, T. (2016). Joint properties of friction welded joint between 6061 Al alloy pipe and Al-Si12CuNi (AC8A) Al cast alloy pipe. The International Journal of Advanced Manufacturing Technology, 86(9): 2603-2614. https://doi.org/10.1007/s00170-016-8348-3
[14] Winiczenko, R., Kaczorowski, M., Skibicki, A. (2018). The microstructures, mechanical properties, and temperature distributions in nodular cast iron friction-welded joint. Journal of the Brazilian Society of Mechanical Sciences and Engineering, 40(7): 347. https://doi.org/10.1007/s40430-018-1261-y
[15] Liu, X., Lan, S., Ni, J. (2014). Analysis of process parameters effects on friction stir welding of dissimilar aluminum alloy to advanced high strength steel. Materials & Design, 59: 50-62. https://doi.org/10.1016/j.matdes.2014.02.003
[16] Coelho, R.S., Kostka, A., Dos Santos, J.F., Kaysser-Pyzalla, A. (2012). Friction-stir dissimilar welding of aluminium alloy to high strength steels: Mechanical properties and their relation to microstructure. Materials Science and Engineering: A, 556: 175-183. https://doi.org/10.1016/j.msea.2012.06.076
[17] Boonchouytan, W., Chatthong, J., Rawangwong, S., Burapa, R. (2014). Effect of heat treatment T6 on the friction stir welded SSM 6061 aluminum alloys. Energy Procedia, 56: 172-180. https://doi.org/10.1016/j.egypro.2014.07.146
[18] Tang, J., Shen, Y. (2017). Effects of preheating treatment on temperature distribution and material flow of aluminum alloy and steel friction stir welds. Journal of Manufacturing Processes, 29: 29-40. https://doi.org/10.1016/j.jmapro.2017.07.005
[19] Karash, E.T., Yassen, S.R., Qasim, M.T.E. (2015). The effect of the cutting depth of the tool friction stir process on the mechanical properties and microstructures of aluminium alloy 6061-T6. American Journal of Mechanics and Applications, 3(5): 33-41. https://doi.org/10.11648/j.ajma.20150305.11
[20] Lee, W.B., Schmuecker, M., Mercardo, U.A., Biallas, G., Jung, S.B. (2006). Interfacial reaction in steel–aluminum joints made by friction stir welding. Scripta Materialia, 55(4): 355-358. http://doi.org/10.1016/j.scriptamat.2006.04.028
[21] Verma, S., Misra, J.P. (2015). A critical review of friction stir welding process. DAAAM International Scientific Book, 249-266. https://doi.org/10.2507/daaam.scibook.2015.22
[22] Deswal, V., Pabla, B.S. (2022). Analysis of preheating effects on friction stir welding of aluminum alloy. Journal of University of Shanghai for Science and Technology, 24(8): 322-334.
[23] Jabbari, M. (2013). Effect of the preheating temperature on process time in friction stir welding of Al 6061-T6. Journal of Engineering, 2013(1): 580805. http://doi.org/10.1155/2013/580805
[24] Patel, M., Patel, M. (2015). A review on effect of preheating on 6061 T-6 AL using friction stir welding by RSM method. Indian Journal of Applied Research, 5(1): 8-19.
[25] Aglan, H.A., Sudan, A., Prayakarao, K.R., Fateh, M. (2013). Effect of preheating temperature on the mechanical and fracture properties of welded pearlitic rail steels. Engineering, 5(11): 837. http://dx.doi.org/10.4236/eng.2013.511101
[26] Sun, Y.F., Shen, J.M., Morisada, Y., Fujii, H. (2014). Spot friction stir welding of low carbon steel plates preheated by high frequency induction. Materials & Design (1980-2015), 54: 450-457. https://doi.org/10.1016/j.matdes.2013.08.071
[27] Rajendran, C., Srinivasan, K., Balasubramanian, V., Balaji, H., Selvaraj, P. (2017). Effect of tool tilt angle on microstructural characteristics of friction stir welded lap joints of AA2014-T6 aluminum alloy joints. Journal of Manufacturing Engineering, 12(3): 120-126. https://www.smenec.org/index.php/1/article/view/157.
[28] Mehta, K.P., Badheka, V.J. (2016). Effects of tilt angle on the properties of dissimilar friction stir welding copper to aluminum. Materials and Manufacturing Processes, 31(3): 255-263. https://doi.org/10.1080/10426914.2014.994754
[29] Ismael, Q.H., Fathi, M.S., Abid, Z.M. (2023). Effect of friction stir welding parameters on welding joint characteristics: A review. SVU-International Journal of Engineering Sciences and Applications, 4(2): 90-97. https://doi.org/10.21608/svusrc.2023.180975.1090
[30] Fallahi, A., Hosseini-Toudeshky, H., Ghalehbandi, S.M. (2014). Effect of heat treatment on mechanical properties of ECAPed 7075 aluminum alloy. Advanced Materials Research, 829: 62-66. https://doi.org/10.4028/www.scientific.net/AMR.829.62
[31] Singh, S.P., George, D.T., Xavier, A.A.J., Raja, G.A. (2023). Effect of heat treatment on the hardness behaviour of the aluminium 6061 alloy. Materials Today: Proceedings. https://doi.org/10.1016/j.matpr.2023.02.345
[32] Kumar, P., Prateek, K.B., Shilpa, M., Kumar, C.C. (2014). (2014). Optimization of heat treatment parameters for the A2024 aluminum alloy using Taguchi's orthogonal array approach. International Journal of Advanced Engineering & Innovative Technology, 1(3): 1-10.
[33] Agboola, J., Anyoku, E., Oladoye, A. (2021). Effects of

cooling rate on the microstructure, mechanical properties and corrosion resistance of 6xxx aluminium alloy. International Journal of Engineering Materials and Manufacture, 6(1): 43-49. https://doi.org/10.26776/ijemm.06.01.2021.04

[34] Arcaleni, R., Zhang, Q., Olofsson, J., Bogdanoff, T., Morri, A., Jarfors, A.E.W., Ceschini, L. (2025). Comparison of tensile properties and fracture mechanisms between primary and secondary rheocast AlSi7Mg aluminum alloys. International Journal of Metalcasting, 19(2). https://doi.org/10.1007/s40962-025-01827-w

[35] Radaj, D., Kopp, S. (2015). Influence of thermal cycles on the mechanical properties of aluminum friction stir welds. Welding in the World, 59(5): 651-660. https://doi.org/10.1007/s40194-015-0271-9

[36] Güleryüz, G., Öztürk, A. (2020). Relationship between friction stir welding parameters and hardness of ferritic carbon steel joints. Journal of Materials Processing Technology, 276: 116380. https://doi.org/10.1016/j.jmatprotec.2020.116380

[37] Mishra, A., Sefene, E.M., Tsegaw, A.A. (2022). Performance evaluation of a machine learning-based algorithm and Taguchi algorithm for the determination of the hardness value of the friction stir-welded AA 6262 joints at a nugget zone. arXiv preprint arXiv:2203.11649. https://doi.org/10.48550/arXiv.2203.11649

[38] Kumara, M., Sinha, A.N. (2025). Effect of tool rotational speed on microstructure and mechanical properties of friction stir weld joints between interstitial free steel and 6351 aluminum alloy. Welding International, 40(2): 59-69. https://doi.org/10.1080/09507116.2025.2563016

[39] Laska, A., Sadeghi, B., Sadeghian, B., Taherizadeh, A., Szkodo, M., Cavaliere, P. (2023). Temperature evolution, material flow, and resulting mechanical properties as a function of tool geometry during friction stir welding of AA6082. Journal of Materials Engineering and Performance, 32: 10655-10668. https://doi.org/10.1007/s11665-023-08671-1

[40] Koch, S.F., Bauer, J., Wagner, H., Horsch, J., Brecht, S., Fleischer, J. (2014). Characterization of an eigenfrequency adaptable machine tool carriage. Procedia CIRP, 14: 412-417. https://doi.org/10.1016/j.procir.2014.03.086

[41] Powałka, B., Tomaszewski, J. (2025). Chatter detection and suppression in CNC lathe. Precision Engineering, 94: 526-544. https://doi.org/10.1016/j.precisioneng.2025.03.022

[42] Liu, J.H., Huang, C.X., Wu, S.D., Zhang, Z.F. (2008). Tensile deformation and fracture behaviors of high purity polycrystalline zinc. Materials Science and Engineering: A, 490(1-2): 117-125. https://doi.org/10.1016/j.msea.2008.01.004

[43] Li, Y., Sun, D., Gong, W. (2019). Effect of tool rotational speed on the microstructure and mechanical properties of bobbin tool friction stir welded 6082-T6 aluminum alloy. Metals, 9(8): 894. https://doi.org/10.3390/met9080894

[44] Zhou, Z., Wen, Z., Su, F. (2026). Thermomechanical flow in aluminum–steel dissimilar joints. Materials Today Communications, 52: 115007. https://doi.org/10.1016/j.mtcomm.2026.115007

[45] Chen, C. (2024). Machine learning-based characterization of friction stir welding in aluminum alloys. Journal of Adhesion Science and Technology, 38(18): 3438-3460. https://doi.org/10.1080/01694243.2024.2345163

[46] Ben Khalifa, R., Toumi, O. (2025). Prediction of FSW temperature and tensile stress for 6061-T6. Proceedings of the Institution of Mechanical Engineers, Part C: Journal of Mechanical Engineering Science, 239(14): 5622-5635. https://doi.org/10.1177/09544062251327542

[47] El-Morsy, A.W., Ghanem, M., Bahaitham, H. (2018). Effect of friction stir welding parameters on the microstructure and mechanical properties of AA2024-T4 aluminum alloy. Engineering, Technology & Applied Science Research, 8(1): 2493-2498. https://doi.org/10.48084/etasr.1704

[48] Pita, M.J. (2023). Investigation of the effect of tool temperature on microstructure, hardness, and wear behaviour of aluminium 6061-T6 alloy welded by the friction stir welding process. Material Design & Processing Communications, 2023: 1-9. https://doi.org/10.1155/2023/1795150

[49] Hu, Y., Niu, Y., Zhao, Y., Yang, W., Ma, X., Li, J. (2022). Friction stir welding of CoCrNi medium-entropy alloy: Recrystallization behaviour and strengthening mechanism. Materials Science and Engineering: A, 848: 143361. https://doi.org/10.1016/j.msea.2022.143361

[50] Zhang, Y., Shi, J., Liao, G., Li, R., Peng, J., Kuang, S., Shen, F. (2025). Effects of tool structure and process parameters in friction stir welding on the temperature and mechanical properties of dissimilar copper– aluminium welded joints. Metals, 15(2): 193. https://doi.org/10.3390/met15020193

[51] Poulia, A., Karantzalis, A.E. (2025). Latest advancements and mechanistic insights into high-entropy alloys: Design, properties and applications. Materials, 18(24): 5616. https://doi.org/10.3390/ma18245616

[52] Genevois, C., Deschamps, A., Denquin, A., Doisneau-Cottignies, B. (2005). Quantitative investigation of precipitation and mechanical behaviour for AA2024 friction stir welds. Acta Materialia, 53(8): 2447-2458. https://doi.org/10.1016/j.actamat.2005.02.007